Published in final edited form as:
J Urol. 2013 October ; 190(4 0): 1596–1602. doi:10.1016/j.juro.2013.01.002.

Physiological Relevance of LL-37 Induced Bladder Inflammation and Mast Cells

Siam Oottamasathien[#*,‡], **Wanjian Jia**[#], **Lindsi McCoard Roundy**, **Jianxing Zhang**, **Li Wang**, **Xiangyang Ye**, **A. Cameron Hill**, **Justin Savage**, **Wong Yong Lee**, **Ann Marie Hannon**, **Sylvia Milner**, and **Glenn D. Prestwich**[‡]
Division of Pediatric Urology (SO, WJ, LMR, LW, ACH, AMH, SM) and Departments of Surgery (SO, WJ, LMR, LW, ACH, AMH, SM), Medicinal Chemistry (JZ, GDP) and Pharmacotherapy (XY) and Center for Therapeutic Biomaterials (JZ, GDP), University of Utah/Primary Children's Medical Center and GlycoMira Therapeutics, L.L.C. (JS, WYL), Salt Lake City, Utah

[#] These authors contributed equally to this work.

Abstract

Purpose—We established the physiological relevance of LL-37 induced bladder inflammation. We hypothesized that 1) human urinary LL-37 is increased in pediatric patients with spina bifida, 2) LL-37 induced inflammation occurs in our mouse model via urothelial binding and is dose dependent and 3) LL-37 induced inflammation involves mast cells.

Materials and Methods—To test our first hypothesis, we obtained urine samples from 56 pediatric patients with spina bifida and 22 normal patients. LL-37 was measured by enzyme-linked immunosorbent assay. Our second hypothesis was tested in C57Bl/6 mice challenged with 7 LL-37 concentrations intravesically for 1 hour. At 24 hours tissues were examined histologically and myeloperoxidase assay was done to quantitate inflammation. In separate experiments fluorescent LL-37 was instilled and tissues were obtained immediately (time = 0) and at 24 hours (time = 24). To test our final hypothesis, we performed immunohistochemistry for mast cell tryptase and evaluated 5 high power fields per bladder to determine the mean number of mast cells per mm^2.

Results—Urinary LL-37 was 89-fold higher in patients with spina bifida. Mouse LL-37 dose escalation experiments revealed increased inflammation at higher LL-37 concentrations. Fluorescent LL-37 demonstrated global urothelial binding at time = 0 but was not visible at time = 24. Immunohistochemistry for tryptase revealed mast cell infiltration in all tissue layers. At higher concentrations the LL-37 challenge led to significantly greater mast cell infiltration.

Conclusions—Urinary LL-37 was significantly increased in pediatric patients with spina bifida. To our knowledge we report for the first time that LL-37 can elicit profound, dose dependent bladder inflammation involving the urothelium. Finally, inflammation propagation involves mast cells.

Keywords

urinary bladder; mast cells; meningomyelocele; cystitis, interstitial; inflammation

[*]Correspondence: University of Utah/Primary Children's Medical Center, 100 North Mario Capecchi Dr., Suite 2200, Salt Lake City, Utah 84113 (siam.oottamasathien@hsc.utah.edu). .
[‡]Financial interest and/or other relationship with GlycoMira Therapeutics.

Inflammatory conditions that afflict the bladder are of significant urological health concern. Our group previously reported a new biologically based, nongenetically manipulated, noninfectious, nonchemically induced mouse bladder inflammation model based on the naturally occurring urinary antimicrobial peptide LL-37.[1]

Inflammatory conditions affecting the bladder can develop in children and adults. In children many diseases can lead to neurogenic bladder conditions, including MM/SB. These processes overlap in adults, in whom chronic inflammatory bladder disorders such as IC/PBS result in debilitating urinary symptoms. To better understand these conditions, novel inflammatory models are needed to further determine mechanisms. These models could also potentially be used to investigate new therapeutic agents. We tested 3 hypotheses to strengthen the physiological relevance of our previously reported LL-37 induced bladder inflammation model.

LL-37 is a host defense peptide produced from the C-terminus of hCAP18 precursor protein and synthesized by diverse cell types, including epithelial cells and circulating neutrophils.[2] Human and mouse urothelial cells naturally produce LL-37.[3] During pediatric UTI (pyelonephritis and/or cystitis), urinary LL-37 is significantly increased.[3] In addition, low LL-37 (13 to 25 μM) is cytotoxic against eukaryotic cells in vitro.[4] Based on these studies, we first hypothesized that urinary LL-37 is increased in pediatric patients with MM/SB. We tested this hypothesis by investigating urinary LL-37 in children with MM/SB and normal pediatric patients.

To expand our initial report, we further hypothesized that LL-37 induced inflammation occurs via urothelial binding and is dose dependent. A goal of this hypothesis was to better elucidate LL-37 spatial and temporal characteristics. To accomplish this, we used biologically active, fluorescently labeled LL-37.

Multiple investigators have described the importance of mast cells in the pathophysiology of inflammatory bladder diseases such as IC/PBS.[5–13] Mast cells are multifunctional immune cells that develop from a specific bone marrow progenitor, migrate into tissue perivascular spaces and can be activated by bacteria, chemicals, kinins and neuropeptides such as substance P and acetylcholine.[13–15] Mast cells have potent mediators that can be pre-synthesized, such as granule stored molecules (eg tryptase, chymase, heparin, histamine, proteases, phospholipases, chemotactic substances and cytokines) or synthesized de novo (eg cytokines, especially interleukin-6, leukotrienes, prostaglandins, nitric oxide and tumor necrosis factor-α).[5,14] Investigators identified mast cell chymase as a possible mediator of neurogenic bladder fibrosis in patients with MM/SB[16] and others noted that LL-37 induces mast cell chemotaxis.[17] Thus, we hypothesized that LL-37 induced bladder inflammation mechanistically involves mast cells.

MATERIALS AND METHODS

Human Urinary LL-37

We obtained appropriate institutional review board approval from the University of Utah and Primary Children's Medical Center. Urine sample collection and storage from pediatric (age less than 18 years) patients with MM/SB (56) and normal nonMM/SB pediatric patients (22) were collected.

1) We performed a urinary dipstick test using Rapid™ Response Urinalysis Reagent strips (U10-1S100). Nitrite and leukocyte positivity were considered positive indicators of active infection and these cases were excluded from study. 2) We then performed urinary LL-37 ELISA using the Human LL-37 ELISA Kit (Hycult®) according to the manufacturer

protocol. Final concentrations were based on a standard curve and are shown in ng/ml. 3) We measured urinary creatinine by diluting samples 1:20 in dilution buffer from the Creatinine Assay Kit (lot 286154, R&D Systems®) and calculated urinary creatinine in mg/ml based on a standard curve. 4) For normalization we divided the LL-37 concentration in ng/ml by creatinine in mg/ml to determine normalized LL-37 in ng/mg creatinine. Statistical analysis was done with the Wilcoxon signed rank test with $p < 0.05$ considered significant.

LL-37 Induced Bladder Inflammation Mouse Model

Experiments were performed in accordance with the University of Utah animal care and use committee in 8 to 12-week-old female C57BL/6 mice. LL-37 was obtained in high performance liquid chromatography homogenous form from the University of Utah Core (peptide sequence LLGDFFRKSKEKIGKEFKRIVQRIKDFLRNLVPRTES) and dissolved in nanopure water. Seven LL-37 concentrations were tested, including 0, 10, 20, 40, 80, 160 and 320 μM, in 4 preparations per concentration. After anesthesia induction, LL-37 was instilled in the mice via catheterization at a volume equal to capacity (150 μl), as previously described,[18–22] with an intravesical time of 1 hour. Substances were infused slowly to avoid vesicoureteral reflux.[18–22] Mice were sacrificed and tissues were obtained at 24 hours (t = 24).

Tissue Collection, Histological Evaluation and Tissue MPO Assay

Bladders were removed and split longitudinally. One section was fixed in 4% paraformaldehyde and the other was processed for tissue MPO. Tissues were processed and MPO assays were performed.[23]

LL-37 Bladder Instillation Spatial and Temporal Characteristics

LL-37 fluorescently labeled with AlexaFluor® 568 was synthesized by adding 3 mg LL-37 and 5 mg N-hydroxysuccinimide in 5 ml deionized H_2O to a solution of 1 mg AlexaFluor 568 carboxylic acid in 2 ml dimethylformamide. pH was adjusted to 4.75 and N,N-diethylaminopropyl carbodiimide (5 mg) was added. The reaction mixture was stirred overnight, and dialyzed twice against 100 mM NaCl solution and once against deionized H_2O. The dialyzed solution was lyophilized to yield 2.5 mg LL-37 AlexaFluor 568 bioconjugate.

LL-37 AlexaFluor 568 bioconjugate (320 μM) was done as described previously. Bladder tissues were harvested immediately (t = 0) after 1 hour of dwell time or at 24 hours (t = 24) from 4 mice per time point. Tissue sections were counterstained with DAPI and imaged with a FV1000 Confocal IX81 microscope (Olympus®).

Immunohistochemistry for Mast Cell Tryptase and Mast Cell Counting

Slides were deparaffinized and rehydrated through xylene and graded alcohols. Endogenous peroxidase activity was blocked with 1% hydrogen peroxide in TBST for 20 minutes. Slides were washed 3 times in TBST for 3 minutes. Antigen retrieval was performed (lot V0421, Vector Laboratories, Burlingame, California). To minimize nonspecific antibody binding, sections were incubated for 60 minutes in 5% fetal bovine serum in TBS with 0.3% Triton™ X-100. Sections were incubated overnight at 4C with primary antibody (rabbit-anti mouse tryptase, 1:800 in blocking solution, lot 32889, Santa Cruz Biotechnology, Santa Cruz, California). After overnight incubation, slides were washed 3 × 3 minutes in TBST. Sections were incubated for 60 minutes with biotinylated secondary antibody (1:2,000), followed by Vectastain® Elite ABC Reagent (lot PK-6100) diluted in TBST for 30 minutes. Between incubations, sections were washed 3 × 3 minutes in TBST. To visualize immunoreactivity, sections were incubated in DAB peroxidase substrate for 22 to 33 seconds. Sections were

washed in double distilled H_2O, counterstained and dehydrated. Negative controls included incubation with TBST in place of the primary antibody with no immunoreactivity observed. Immunofluorescence experiments were done with DyLight® 633 secondary antibody (goat anti-rabbit IgG, 1:800 dilution, No. 35562).

To count mast cells, a single reviewer chose 5 random high power fields (40× magnification) for each tissue chip and counted all DAB tryptase positive cells, yielding an average mast cell number per mm^2 per sample. Statistical analysis was done with ANOVA. Multiple comparisons were made using the Bonferroni adjustment with $p < 0.05$ considered significant.

RESULTS

Human Urinary LL-37

Our first hypothesis was that human urinary LL-37 would be increased in pediatric patients with MM/SB. In 56 children with MM/SB average ± SD urinary LL-37 was 20.43 ± 132.12 ng/mg (median 0.401, range 0.024 to 987.87). In 22 normal children average LL-37 was 0.23 ± 0.39 ng/mg (median 0.0325, range 0 to 1.6). When mean values were compared, results revealed an 89-fold increase in urinary LL-37 in children with MM/SB ($p < 0.001$) and a 12.3-fold increase using median values.

LL-37 Induced Bladder Inflammation Mouse Model-Dose Response

The results of testing our second hypothesis revealed that LL-37 induces bladder inflammation in dose-response fashion. Gross inspection showed no evidence of inflammation in controls with severe inflammation, consisting of global erythema, hemorrhage and severe tissue edema, for the 320 μM LL-37 challenge (fig. 1, *A* and *G*). These findings were consistent with those previously reported.[1] Gross inspection revealed a steady increase in erythema, hemorrhage and tissue edema with increasing LL-37 (fig. 1, *B* to *F*). Histology confirmed the gross results with more severe urothelial ulceration and edema, and increased inflammatory cell infiltrate (eg polymorphonuclear leukocytes/mast cells) at higher LL-37 concentrations (fig. 1, *H* to *N*). No evidence of inflammation was observed in controls and inflammation levels were consistent in each group.

We determined inflammation using tissue MPO, a quantitative method to investigate neutrophil activity via the MPO enzyme in neutrophils. Comparison of LL-37 challenged tissues showed minimal MPO activity in saline controls (1.6 ng/mg), and for the LL-37 challenge at 10, 20 and 40 μM (0.6, 1.8 and 1.3 ng/mg, respectively, fig. 2). Increased MPO was observed at 80, 160 and 320 μM LL-37 (4.6, 28.4 and 77.9 ng/mg, respectively). Results at 320 μM were consistent with our previously published findings (vs all other concentrations $p < 0.0001$).[1]

LL-37 Showed Urothelial Binding

To elucidate the spatial and temporal characteristics of LL-37 activity, we instilled 320 μM fluorescent LL-37 and harvested tissues immediately ($t = 0$) or at 24 hours ($t = 24$). Controls showed no evidence of fluorescence except from the expected DAPI nuclear counterstain (fig. 3, *A*). At $t = 0$ a uniform GAG layer coating and global urothelial penetration were noted but there was no evidence of deeper penetration (fig. 3, *B*). Results in the 24-hour group revealed no LL-37 in any tissue layer (fig. 3, *C*). Tissues showed the typical inflammatory phenotype, confirming the retained biological properties of fluorescent LL-37 (data not shown).

Mast Cell Involvement

To determine mast cell involvement in our LL-37 model, we performed immunohistochemistry for mast cell tryptase using a DAB and immunofluorescence approach to increase mast cell detection. Figure 4 shows saline controls vs 320 μM LL-37 challenged tissues. No evidence of mast cell tryptase staining was observed in controls (fig. 4, *A* and *C*). In 320 μM LL-37 challenged tissues substantial mast cell infiltration was noted in all tissue layers (fig. 4, *B* and *D*). Immunofluorescence staining demonstrated potential degranulation of tryptase in the endovasculature (fig. 4, *D*).

Using these tissues, we quantified mast cells across all LL-37 challenge concentrations to further determine whether LL-37 induces a dose response profile for mast cell infiltration. Specific numbers of mast cells were determined for the urothelium and submucosa, including the lamina propria, as well as for detrusor smooth muscle layers. Similar to our previous MPO results, few mast cells infiltrated between tissues at 0 (control), 10, 20 or 40 μM LL-37 (fig. 5). Minimal differences were observed between the urothelial/submucosa and detrusor smooth muscle layers. A clear increase in the number of mast cells was seen in urothelial/submucosa and detrusor smooth muscle at 80 μM (20.09 and 7.21 mast cells per mm^2) with a steady increase at 160 μM (23.14 and 13.97 mast cells per mm^2), peaking at 320 μM LL-37 (40.17 and 28.60 mast cells per mm^2, respectively, fig. 5). When we directly compared results in LL-37 challenged tissues at 320 vs 0 μM in controls, we noted a 26.3-fold increase in mast cells in the urothelial/submucosa layer and a 14.5-fold increase in the detrusor smooth muscle layer of challenged tissues ($p = 0.0004$ and 0.0158, respectively).

DISCUSSION

To strengthen the physiological relevance of our previously described LL-37 induced bladder inflammation model,[1] we tested 3 hypotheses. We first hypothesized that human urinary LL-37 would be increased in pediatric patients with MM/SB. Results revealed an 89-fold increase in urinary LL-37 in pediatric patients with MM/SB. The etiology remains unclear, especially in the face of negative urinalyses for an active UTI. Previous investigators concluded that LL-37 is produced by urothelial cells and significantly increases during episodes of active kidney and/or bladder infection.[3] Our working theory for increased LL-37 in pediatric patients with neurogenic bladder is that chronic urinary distention and stasis cause an insult to the underlying urothelium, resulting in up-regulation of LL-37 synthesis and liberation. Investigators reported that LL-37 is cytotoxic to cells at micromolar concentrations.[4] Therefore, the clinical correlation for the observed increase warrants further investigation.

Using our mouse model, we further hypothesized that LL-37 induces inflammation via urothelial binding and is dose dependent. Results showed robust GAG layer coating and urothelial binding of LL-37, which this vanished after 24 hours. These findings suggest that the inflammatory insult extends beyond the initial exposure. Also, the inflammatory phenotype is in part propagated by the recruitment of active inflammatory cells (eg neutrophils, mast cells and monocytes/macrophages) of the innate immune system. LL-37 is a direct chemoattractant for neutrophils, mast cells, monocytes/macrophages and T cells.[17,24] This active recruitment could explain the prolonged inflammation observed.

Our data also indicated robust LL-37 urothelial binding and studies showed that LL-37 can be cytotoxic at low concentrations.[4] Thus, injury to the underlying urothelium could involve apoptotic mechanisms. Histology in IC/PBS cases revealed apoptosis as a key finding underlying urothelial cell injury and pathogenesis.[25–27] Further investigation is warranted of the role of LL-37 in urothelial cell injury.

Our results indicate that the level of inflammation was dose dependent. With each increase in the LL-37 challenge, inflammation increased histologically and quantitatively on tissue MPO assays. These results highlight the advantage of a dose-response model with potential use for investigating new anti-inflammatory therapies. Assessing the therapeutic efficacy of novel drugs at variable inflammatory severity levels would be advantageous.

Multiple studies highlight the importance of mast cells in the pathophysiology of inflammatory bladder diseases, such as IC/PBS.[5–13] Therefore, we formulated a final hypothesis that LL-37 induced bladder inflammation mechanistically involves mast cells. We noted a key dose-response relationship between LL-37 challenged tissues, and the active recruitment and infiltration of mast cells. The higher the LL-37 challenge, the greater the number of mast cells observed in all tissue layers. Kastrup et al previously described a mast cell count of greater than 20 cells per mm^2 in bladder tissue samples of patients with IC/PBS.[28] Our results showed greater than 20 mast cells per mm^2 in the urothelial and submucosa layer at LL-37 concentrations of greater than 80 μM. At the 320 μM LL-37 challenge the detrusor smooth muscle layer showed greater than 20 mast cells per mm^2. These findings solidify the physiological relevance of this model, mimicking that observed in human disease. In addition, mast cells are implicated in the neurogenic bladder fibrosis seen in MM/SB and fibrotic events in patients with IC/PBS.[16,29] No clinically available compounds exist that effectively block mast cell activation[11] but therapeutic promise remains.

CONCLUSIONS

Urinary LL-37 was significantly increased in pediatric patients with SB. In our mouse model a naturally based biological compound elicited profound dose dependent bladder inflammation. Also, LL-37 appeared to elicit inflammation through a urothelial mechanism. Finally, inflammation propagation intimately involved mast cells. To our knowledge these findings represent the first biological, noninfectious, nonchemically induced bladder inflammation model that is physiologically relevant.

Acknowledgments

Study received approval from the University of Utah and Primary Children's Medical Center institutional review board, and University of Utah animal care and use committee.

Supported by National Institute of Diabetes and Digestive and Kidney Diseases Grant NIH SBIR 1R43DK093413 (SO, GDP, JS, JZ), and the NIH K12 Career Development Award in Children's Health Research UL1RR025764 (SO) from the University of Utah Center for Clinical and Translational Sciences, and National Center for Advancing Translational Sciences, American Urological Association/Pfizer Benign Urological Diseases Award (SO), Primary Children's Medical Center Foundation Integrated Science Award (SO, GDP) and Primary Children's Medical Center Foundation Early Career Development Award (SO).

Abbreviations and Acronyms

DAB	diaminobenzidine
ELISA	enzyme-linked immunosorbent assay
GAG	glycosaminoglycan
IC/PBS	interstitial cystitis/painful bladder syndrome
MM/SB	myelomeningocele/spina bifida
MPO	myeloperoxidase

TBS	tris buffered saline
TBST	TBS-Tween®
t	time
UTI	urinary tract infection

REFERENCES

1. Oottamasathien S, Jia W, McCoard L, et al. A murine model of inflammatory bladder disease: cathelicidin peptide induced bladder inflammation and treatment with sulfated polysaccharides. J Urol. 2011; 186:1684. [PubMed: 21855919]
2. Nijnik A, Hancock RE. The roles of cathelicidin LL-37 in immune defences and novel clinical applications. Curr Opin Hematol. 2009; 16:41. [PubMed: 19068548]
3. Chromek M, Slamova Z, Bergman P, et al. The antimicrobial peptide cathelicidin protects the urinary tract against invasive bacterial infection. Nat Med. 2006; 12:636. [PubMed: 16751768]
4. Johansson J, Gudmundsson GH, Rottenberg ME, et al. Conformation-dependent antibacterial activity of the naturally occurring human peptide LL-37. J Biol Chem. 1998; 273:3718. [PubMed: 9452503]
5. Batler RA, Sengupta S, Forrestal SG, et al. Mast cell activation triggers a urothelial inflammatory response mediated by tumor necrosis factor-alpha. J Urol. 2002; 168:819. [PubMed: 12131374]
6. Klumpp DJ, Rudick CN. Summation model of pelvic pain in interstitial cystitis. Nature clinical practice. Urology. 2008; 5:494. [PubMed: 18769376]
7. Larsen MS, Mortensen S, Nordling J, et al. Quantifying mast cells in bladder pain syndrome by immunohistochemical analysis. BJU Int. 2008; 102:204. [PubMed: 18384636]
8. Pang X, Sant G, Theoharides TC. Altered expression of bladder mast cell growth factor receptor (c-kit) in interstitial cystitis. Urology. 1998; 51:939. [PubMed: 9609630]
9. Peeker R, Enerback L, Fall M, et al. Recruitment, distribution and phenotypes of mast cells in interstitial cystitis. J Urol. 2000; 163:1009. [PubMed: 10688040]
10. Rudick CN, Bryce PJ, Guichelaar LA, et al. Mast cell-derived histamine mediates cystitis pain. PLoS One. 2008; 3:e2096. [PubMed: 18461160]
11. Sant GR, Kempuraj D, Marchand JE, et al. The mast cell in interstitial cystitis: role in pathophysiology and pathogenesis. Urology. 2007; 69:34. [PubMed: 17462477]
12. Spanos C, Pang X, Ligris K, et al. Stress-induced bladder mast cell activation: implications for interstitial cystitis. J Urol. 1997; 157:669. [PubMed: 8996395]
13. Theoharides TC, Kempuraj D, Sant GR. Mast cell involvement in interstitial cystitis: a review of human and experimental evidence. Urology. 2001; 57:47. [PubMed: 11378050]
14. Galli SJ. New concepts about the mast cell. N Engl J Med. 1993; 328:257. [PubMed: 8418407]
15. Galli SJ, Nakae S, Tsai M. Mast cells in the development of adaptive immune responses. Nat Immunol. 2005; 6:135. [PubMed: 15662442]
16. Howard PS, Renfrow D, Schechter NM, et al. Mast cell chymase is a possible mediator of neurogenic bladder fibrosis. Neurourol Urodyn. 2004; 23:374. [PubMed: 15227657]
17. Niyonsaba F, Iwabuchi K, Someya A, et al. A cathelicidin family of human antibacterial peptide LL-37 induces mast cell chemotaxis. Immunology. 2002; 106:20. [PubMed: 11972628]
18. Bjorling DE, Jerde TJ, Zine MJ, et al. Mast cells mediate the severity of experimental cystitis in mice. J Urol. 1999; 162:231. [PubMed: 10379792]
19. Gonzalez RR, Fong T, Belmar N, et al. Modulating bladder neuro-inflammation: RDP58, a novel anti-inflammatory peptide, decreases inflammation and nerve growth factor production in experimental cystitis. J Urol. 2005; 173:630. [PubMed: 15643278]
20. Saban MR, Nguyen NB, Hammond TG, et al. Gene expression profiling of mouse bladder inflammatory responses to LPS, substance P, and antigen-stimulation. Am J Pathol. 2002; 160:2095. [PubMed: 12057914]

21. Saban MR, Saban R, Hammond TG, et al. LPS-sensory peptide communication in experimental cystitis. Am J Physiol Renal Physiol. 2002; 282:F202. [PubMed: 11788433]
22. Saban R, Gerard NP, Saban MR, et al. Mast cells mediate substance P-induced bladder inflammation through an NK(1) receptor-independent mechanism. Am J Physiol Renal Physiol. 2002; 283:F616. [PubMed: 12217852]
23. Zhang J, Xu X, Rao NV, et al. Novel sulfated polysaccharides disrupt cathelicidins, inhibit RAGE and reduce cutaneous inflammation in a mouse model of rosacea. PLoS One. 2011; 6:e16658. [PubMed: 21347371]
24. Yang D, Chertov O, Oppenheim JJ. Participation of mammalian defensins and cathelicidins in anti-microbial immunity: receptors and activities of human defensins and cathelicidin (LL-37). J Leukocyte Biol. 2001; 69:691. [PubMed: 11358975]
25. Kutlu O, Akkaya E, Koksal IT, et al. Importance of TNF-related apoptosis-inducing ligand in pathogenesis of interstitial cystitis. Int Urol Nephrol. 2010; 42:393. [PubMed: 19705295]
26. Shie JH, Liu HT, Kuo HC. Increased cell apoptosis of urothelium mediated by inflammation in interstitial cystitis/painful bladder syndrome. Urology. 2012; 79:484 e7. [PubMed: 22310775]
27. Yamada T, Nishimura M, Mita H. Increased number of apoptotic endothelial cells in bladder of interstitial cystitis patients. World J Urol. 2007; 25:407. [PubMed: 17554544]
28. Kastrup J, Hald T, Larsen S, et al. Histamine content and mast cell count of detrusor muscle in patients with interstitial cystitis and other types of chronic cystitis. Br J Urol. 1983; 55:495. [PubMed: 6626895]
29. Richter B, Roslind A, Hesse U, et al. YKL-40 and mast cells are associated with detrusor fibrosis in patients diagnosed with bladder pain syndrome/interstitial cystitis according to the 2008 criteria of the European Society for the Study of Interstitial Cystitis. Histopathology. 2010; 57:371. [PubMed: 20840668]

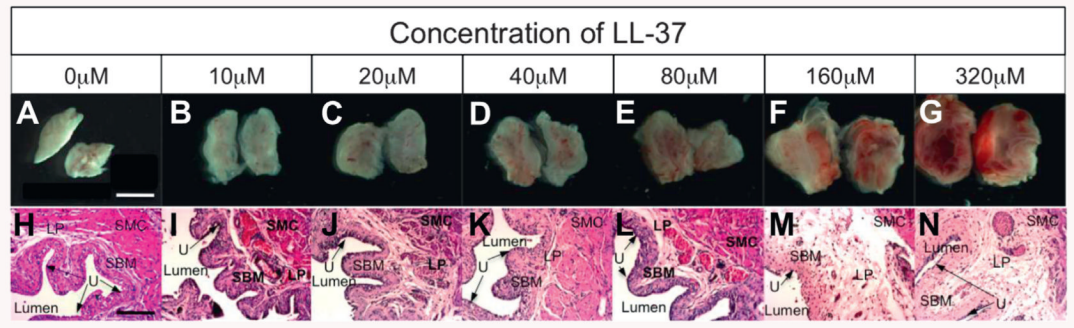

Figure 1.

LL-37 challenge dose response. Gross images show hemisected bladders with inner mucosal surface visualized (*A* to *G*). Representative histological images reveal increasing inflammation with higher LL-37 challenge (*H* to *N*). *LP*, lamina propria. *SMC*, submucosa. *SBM*, bladder smooth muscle. *U*, urothelium. Scale bars represents 0.5 (*A*) and 150 (*H*) μM. H|&|E, reduced from ×10.

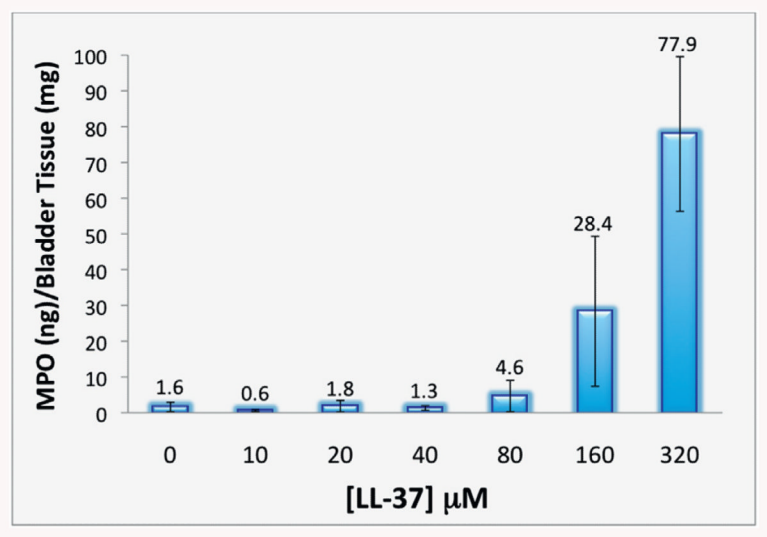

Figure 2.
Increasing MPO was observed with higher LL-37 in LL-37 dose response challenged tissues.

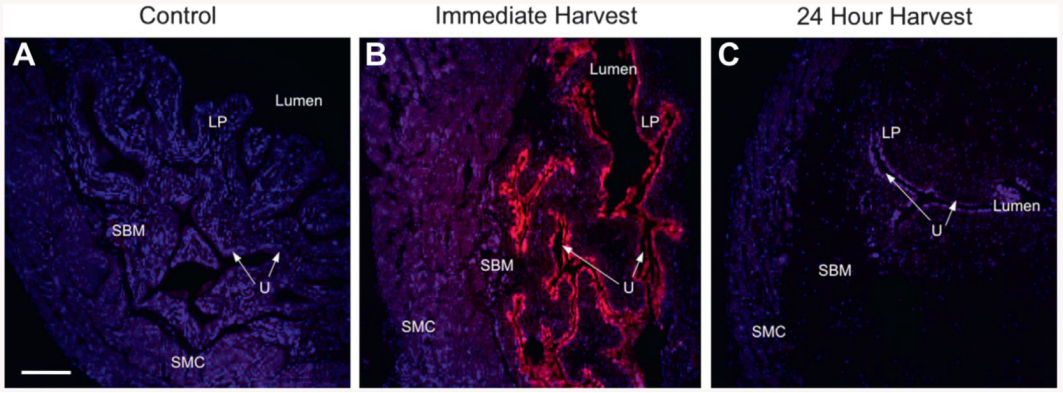

Figure 3.

Instillation of 320 μM fluorescence labeled LL-37 (pink areas) in control (*A*), and at immediate (*B*) and 24-hour (*C*) harvest after 1-hour instillation. Global GAG layer coating and urothelial binding were observed after immediate harvest but there was no evidence of fluorescent LL-37 after 24-hour harvest. *LP*, lamina propria. *SBM*, bladder smooth muscle. *U*, urothelium. *SMC*, submucosa. Scale bar represents 150 μM (*A*). Reduced from ×10.

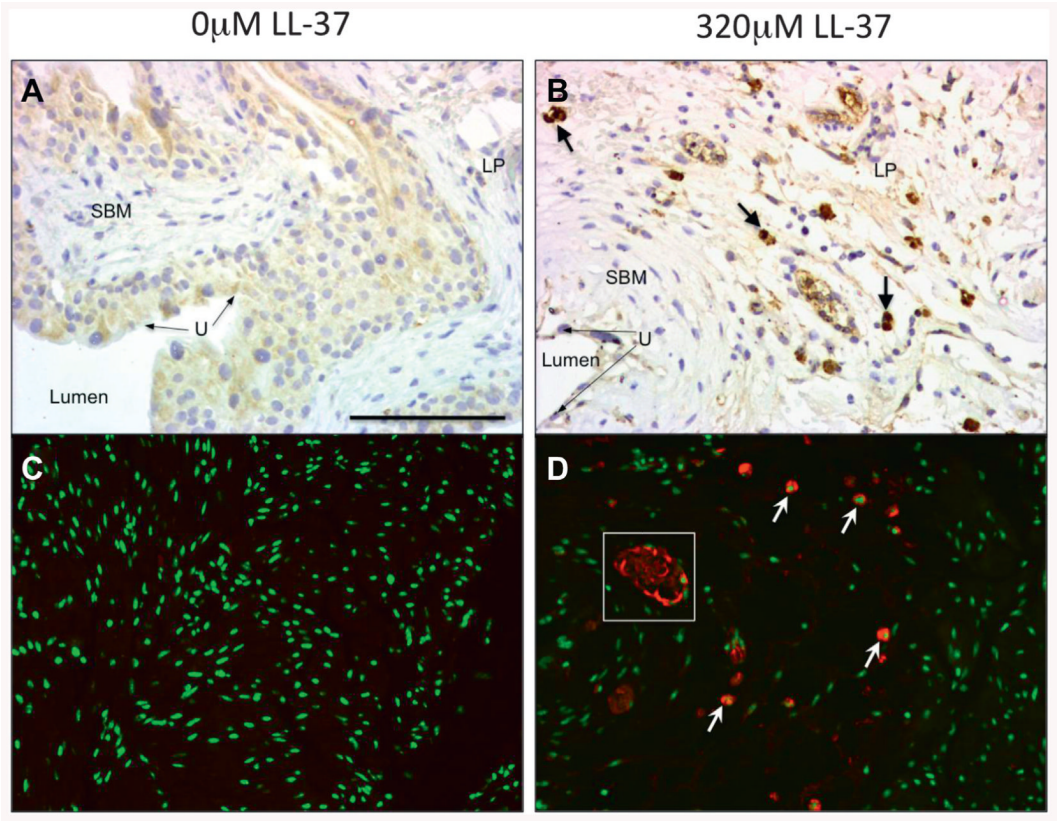

Figure 4.

Immunohistochemistry for mast cell tryptase. Brown areas represent mast cell detection (*A* and *B*). *LP*, lamina propria. *SBM*, bladder smooth muscle. *U*, urothelium. DAB stain, reduced from ×20. Immunofluorescence (*C* and *D*). Red areas represent mast cell detection. No evidence of mast cell presence in nonchallenged tissues (*A* and *C*). Robust mast cells in LL-37 challenged tissues (*B* and *D*). Arrows indicate mast cell samples. White square indicates representative tryptase degranulation pattern in endovasculature. Scale bar represents 75 μM (*A*). Reduced from ×20.

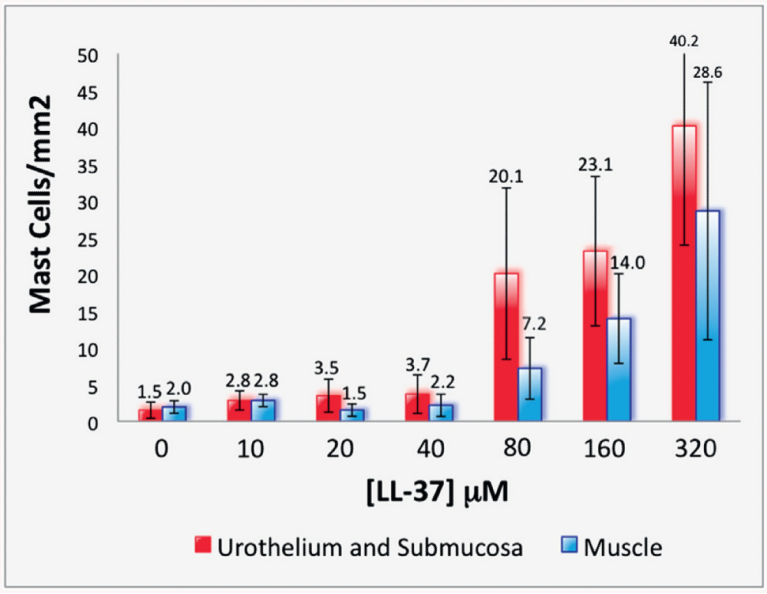

Figure 5.
Quantitation of mast cell numbers in LL-37 dose response challenged tissues. Red bars represent urothelium and submucosa. Blue bars represent muscle.